Short Papers

A Simple Metric for Slew Rate of *RC* Circuits Based on Two Circuit Moments

Kanak Agarwal, Dennis Sylvester, and David Blaauw

***Abstract*—In this paper, we introduce a simple metric for the slew rate of an *RC* circuit based on the first two circuit moments. Metrics focusing on 50% delay of *RC* circuits have been proposed recently that greatly improve the accuracy of the traditional Elmore delay model. However, these new models have not been applied to the determination of transition time or slew rates (e.g., 10–90% of V_{dd}). We study how well existing approaches to 50% delay modeling translate to slew-rate modeling. We first describe a new metric called slew with two moments (S2M) that is based on Elmore's observation that the transition time of a step response is proportional to the standard deviation of the corresponding impulse response. The S2M metric modifies Elmore's original formulation by deriving a new constant of proportionality. This new constant is shown to be more accurate for general *RC* circuits. Next, we show that metrics relying on a simple constant multiplied by standard deviation such as S2M and Elmore do not work well for near-end nodes. To address this issue, we propose a new slew metric called *scaled S2M* that provides high accuracy across all types of nodes, while maintaining the advantage of a simple closed-form expression. Scaled S2M is shown to be very accurate for both near and far-end nodes. The average error for scaled S2M is approximately 2% with 96% of all nodes showing less than 5% error from a large set of industrial 0.18-μm microprocessor nets.**

***Index Terms*—Integrated circuit interconnect, interconnect delay, performance optimization, RC trees, slew, timing analysis.**

I. Introduction

The advancement of process technologies to nanometer-scale feature sizes has resulted in large interconnect delays that consume a large fraction of the overall path delay. On-chip interconnects are typically modeled as *RC* circuits and substantial effort has been devoted to the delay prediction of such circuits. Many of the most common delay metrics are based on an analogy between the nonnegative impulse response of an *RC* circuit and probability density functions (PDFs). This analogy stems from the fact that the impulse response $h(t)$ of an *RC* circuit (without a resistive path to the ground) satisfies the following two conditions [1]:

$$h(t) \geq 0 \quad \forall t$$
$$\int_0^\infty h(t)dt = 1. \tag{1}$$

Since these are sufficient conditions for a function to be a PDF, the impulse response of an RC circuit is a PDF. Also, since the step response is the integral of the impulse response, the step response of an *RC* circuit can therefore be modeled as a cumulative density function (CDF). The median of a PDF is defined such that it corresponds to the 50% point of its CDF; hence the 50% delay of an *RC* circuit under step excitation can be calculated accurately by computing the median of the impulse response. However, it is not trivial to compute the median of many PDFs and hence Elmore proposed using the mean of this impulse response to model the 50% delay [2]. Later, it was shown that the mean of an *RC* impulse response is always greater than or equal to its median, and hence Elmore delay is an upper bound on *RC* delay [3]. The mean of the impulse response is given by the first circuit moment (described later in Section II) and is very simple to compute. This has led to the widespread popularity of the Elmore delay metric for performance optimization and delay calculation. However, Elmore delay has been shown to be highly inaccurate in many cases since it does not consider resistive shielding of downstream capacitance [18].

To enhance delay model accuracy, various model-order reduction techniques based on moment matching or the Krylov subspace method were developed and have been widely used in interconnect analysis [4]–[6]. One such technique is called asymptotic waveform evaluation (AWE) and approximates the response of an *RC* interconnect using a reduced-order model by matching the first few circuit moments [4], [7]. The circuit moments are defined as the coefficients of a Taylor expansion of the impulse response at $s = 0$. These moments contain useful information about circuit behavior and can be computed efficiently by path tracing of *RC* or even *RLC* trees [19]. Though model-order reduction techniques provide very high accuracy, their use in the inner optimization loop during the design phase is limited due to a lack of computationally efficient closed-form expressions. Various two-pole delay metrics based on higher-order moments have been proposed to compromise between a complex reduced order model and a simple first moment-based Elmore approximation [8], [9]. These metrics attempt to find a closed form solution of a two-pole approximation, but are generally lacking in accuracy [10]. An empirical delay metric called delay with two moments (D2M) was proposed in [10] and shown to be highly accurate and efficient.

In [11]–[13], the authors extended the probability interpretation of the impulse response of an *RC* circuit by fitting it to the PDF of various statistical distributions. Though these approaches show very high accuracy, they are not as efficient as D2M and require preconstructed look-up tables for delay calculation.

Although there has been a large amount of work focused on accurately modeling 50% delay as described above, the importance of a comparable slew metric has been underemphasized. Modeling transition-time degradation in *RC* circuits is an important part of modeling propagation delay. In static timing analysis, the input to an *RC* network is usually modeled as a saturated ramp. The transition time of this ramp should be considered in interconnect-delay estimation and must also be propagated to fanout stages since gate and interconnect delays have significant sensitivity to the input slews. Noise glitches and their impact on timing due to coupling capacitance also strongly depend on the transition times of aggressor nets. Accurate crosstalk noise modeling therefore requires precise knowledge of the aggressor slews at the location of coupling. The slew metrics currently available in the literature are the Elmore metric [2], Bakoglu's metric [15], and the recently proposed Lognormal metric [20]. Bakoglu's slew metric $(\ln 9 * \text{Elmore})$ is derived from a single dominant pole approximation and is therefore only as accurate as the first order delay metrics. In this paper, we propose a new two-moment based slew metric called scaled slew with two moments (S2M), that is highly accurate and efficient enough for use in physical design optimization loops. Our metric is based on the observation made by Elmore [2] and Gupta [3] that the transition time of an

---

Manuscript received September 13, 2003; revised January 3, 2004. This paper was recommended by Associate Editor S. Sapatnekar.

The authors are with the Department of Electrical Engineering and Computer Science, University of Michigan, Ann Arbor, MI 48109 USA (e-mail: agarwalk@engin.umich.edu).

Digital Object Identifier 10.1109/TCAD.2004.833607

0278-0070/04$20.00 © 2004 IEEE

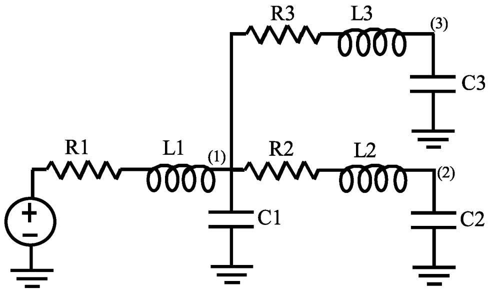

First circuit moments:

$$m_1^1 = -R1(C1 + C2 + C3)$$
$$m_1^2 = -R1(C1 + C2 + C3) - R2C2$$
$$m_1^3 = -R1(C1 + C2 + C3) - R3C3$$

Second circuit moments:

$$m_2^1 = -R1(C1 \times m_1^1 + C2 \times m_1^2 + C3 \times m_1^3) - L1(C1 + C2 + C3)$$
$$m_2^2 = -R1(C1 \times m_1^1 + C2 \times m_1^2 + C3 \times m_1^3) - R2(C2 \times m_1^2) - L1(C1 + C2 + C3) - L2C2$$
$$m_2^3 = -R1(C1 \times m_1^1 + C2 \times m_1^2 + C3 \times m_1^3) - R3(C3 \times m_1^3) - L1(C1 + C2 + C3) - L3C3$$

Fig. 1. Example calculations of the first two circuit moments for a simple *RLC* tree.

RC circuit is similar to the standard deviation of the impulse response. Since some existing delay metrics can be extended to compute slews, we perform a thorough investigation of the accuracy of various slew metrics for the first time. The results imply scaled S2M exhibits much higher accuracy than Bakoglu, Elmore, Weibull, and D2M and is comparable to the more complex Lognormal metric.

II. BACKGROUND

The new slew metric is derived using a probability interpretation of the impulse response; hence we begin by briefly reviewing some concepts of circuit moments and probability moments.

Let $h(t)$ be the impulse response of an *RC* circuit and $H(s)$ be the Laplace transform of $h(t)$. From the definition of circuit moments, we have

$$H(s) = m_0 + m_1 s + m_2 s^2 + m_3 s^3 + \ldots = \sum_{k=0}^{\infty} m_k s^k. \quad (2)$$

Also, since $H(s)$ is the Laplace transform of $h(t)$

$$H(s) = \int_0^{\infty} h(t) e^{-st} dt = \sum_{k=0}^{\infty} \frac{(-1)^k}{k!} s^k \int_0^{\infty} t^k h(t) dt. \quad (3)$$

The kth probability moment $\hat{m}_k$ is defined as

$$\hat{m}_k = \int_0^{\infty} t^k h(t) dt. \quad (4)$$

By comparing (2) and (3) and using the above definition of the probability moments, the relationship between the circuit moments m_k and the probability moments $\hat{m}_k$ can be expressed as

$$m_k = \frac{(-1)^k}{k!} \hat{m}_k. \quad (5)$$

The circuit moments of an *RLC* tree can be computed efficiently by path tracing [19]. The pth order circuit moment $(p > 1)$ of node i (m_p^i) in an *RLC* tree can be expressed as

$$m_p^i = \sum_k \left(-R_{ik} C_k m_{p-1}^i - L_{ik} C_k m_{p-2}^i \right). \quad (6)$$

Here, the summation is taken over all nodes other than the source node. C_k is the capacitance at node k and $R_{ik}(L_{ik})$ denotes the total overlap resistance (inductance) in the unique paths from the source node to nodes i and k. Example calculations of the first two circuit moments for a simple *RLC* tree are shown in Fig. 1.

The circuit moments can be computed recursively using (6). Since circuit moments are related to the probability moments, important information about the *RC* impulse response PDF can be obtained from these circuit moments. The probability moments discussed earlier are the moments about zero. The first probability moment, which is the negative of the first circuit moment, represents the *mean* (μ) of a PDF. Higher order probability moments of the distribution are usually translated into *central moments*. The central moments are the moments around the mean and they contain important geometrical information about the PDF. The kth central moment of a PDF $h(t)$ with mean μ can be expressed as

$$\mu_k = \int_0^{\infty} (t - \mu)^k h(t) dt. \quad (7)$$

Using the above definition of central moments, the first few central moments can be expressed in terms of circuit moments.

$$\begin{aligned} \mu_2 &= 2m_2 - m_1^2 \\ \mu_3 &= -6m_3 + 6m_1 m_2 - 2m_1^3. \end{aligned} \quad (8)$$

Here, μ_2 represents the *variance* of the distribution. It is a measure of the spread or dispersion of the curve from the center. The third central moment μ_3 is a measure of the *skewness* of the distribution.

III. SCALED S2M SLEW METRIC

In this section, we first derive a simple slew metric called S2M. This metric is based on exploiting the relationship between the 10%–90% transition time of an *RC* step response and the standard deviation of the corresponding impulse response. We will show that this metric is accurate only for far-end nodes. We then propose a modified metric called scaled S2M, which builds upon S2M to dramatically improve near-end accuracy.

A. Metric Derivation

The central moments of a PDF define its shape characteristics. Focusing on the slew rate, variance is the most important central mo-

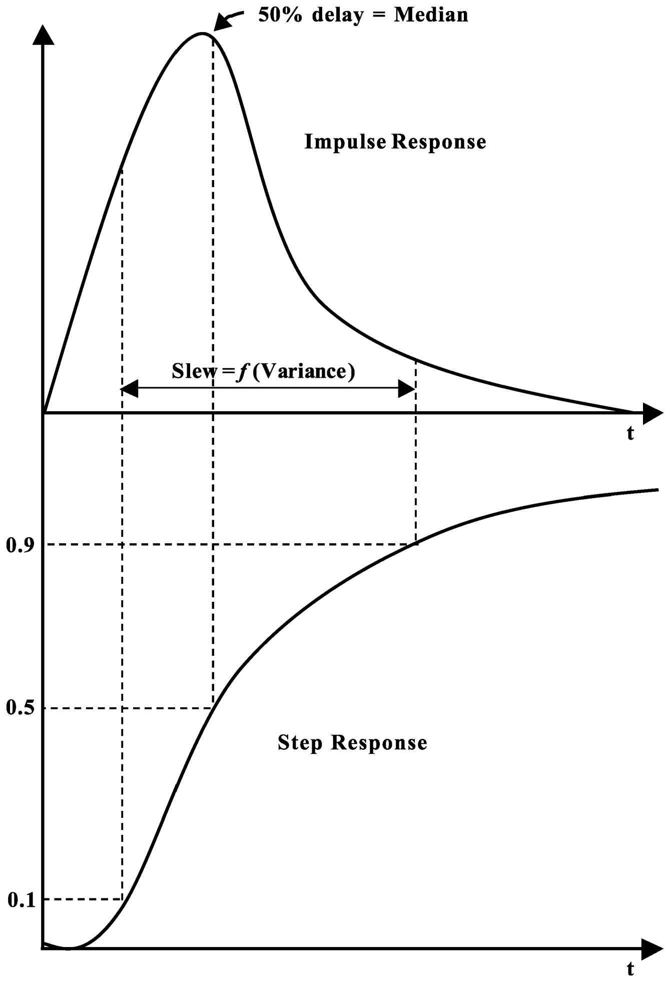

Fig. 2. *RC* impulse response PDF and its corresponding cumulative distribution function (CDF). 50% delay corresponds to the median and 10%–90% slew is a function of the variance of the impulse response.

ment as it represents the spread around the mean. Fig. 2 shows an *RC* impulse response PDF and its corresponding step response CDF. The figure shows that 50% delay corresponds to the median of the impulse response. The figure also shows that 10%–90% slew is a function of variance as it represents the spread of the impulse response [3]. This point supplies the basis for the new metric.

Since the step response of an *RC* circuit is a CDF, it can be modeled by any monotonic function F(t) that satisfies the following conditions:

$$\begin{aligned} &0 \le F(t) \le 1 \quad \forall t \\ &\operatorname*{Lim}_{t->-\infty} F(t) = 0 \\ &\operatorname*{Lim}_{t->\infty} F(t) = 1. \end{aligned} \tag{9}$$

RC responses resemble an exponential waveform; hence we model the step response CDF as

$$F(t) = 1 - e^{\frac{-t}{\tau_r}}. \tag{10}$$

The PDF of the impulse response $h(t)$ corresponding to this CDF (step response) can be obtained as

$$h(t) = \frac{d}{dt}F(t) = \frac{1}{\tau_r}e^{\frac{-t}{\tau_r}}. \tag{11}$$

The mean μ and the variance $\mu_2 (= \sigma^2)$ of this impulse response PDF can be easily computed

$$\begin{aligned} \mu &= \int_0^\infty \frac{t}{\tau_r} e^{\frac{-t}{\tau_r}} dt = \tau_r \\ \mu_2 &= \int_0^\infty (t-\mu)^2 \frac{e^{\frac{-t}{\tau_r}}}{\tau_r} dt = \tau_r^2. \end{aligned} \tag{12}$$

We have one unknown parameter τ_r and can obtain its value by matching the variance in (12) with the variance of the actual *RC* circuit impulse response in (8). This is the key step in our approach because variance is a measure of slew and thus it must be preserved for accurate slew analysis. This differs from traditional delay metrics, which are usually based on matching the mean of the impulse response

$$\tau_r = \sqrt{2m_2 - m_1^2}. \tag{13}$$

This value of τ_r can be substituted in (10) and the step response function F(t) can be solved for 10 and 90% points. The resulting slew metric is given by

$$\mathrm{S2M} = (\ln 9)\left(\sqrt{2m_2 - m_1^2}\right). \tag{14}$$

Regarding the stability of S2M, it can be seen from the definition of the second central moment (variance) in (7) that it is positive for any PDF. Hence the square root term in (13) and (14) is always defined and the metric is stable.[1]

We point out here that if we obtain τ_r by matching just the first moment, we obtain a dominant pole approximation where the dominant pole is the inverse of the Elmore term. The scaled Elmore delay $(\ln 2 * \mathrm{Elmore})$ and Bakoglu's slew metric $(\ln 9 * \mathrm{Elmore})$ are based on this dominant pole approximation. It should also be noted that we do not propose F(t) as a complete output waveform model and solving F(t) for 50% delay may not provide accurate results. Our goal is only to find an accurate and simple closed-form slew metric. For delay calculations, any two moment-based delay metric such as D2M can be used. In fact, using S2M in conjunction with D2M provides a very efficient way to compute delays and slews without complex modeling of the output waveform. In static timing analysis, we are interested only in 50% delay and 10%–90% slew, rather than the exact waveform shape. Complex modeling approaches, such as h-gamma [12] and AWE, attempt to capture the entire output waveform shape, but when these waveforms are propagated to the next stages, they are approximated as saturated ramps; hence the extra computational cost of such approaches is difficult to justify.

It should be noted that the form of S2M in (14) is similar to the rise time metric proposed by Elmore [2]. The only difference between S2M and Elmore's metric is in the constant of proportionality. In Elmore's metric, the constant of proportionality is $\sqrt{2\pi}$ (for a 0%–100% transition) instead of (ln 9) in the S2M metric. The constant $\sqrt{2\pi}$ becomes equal to 2 for 10%–90% transitions. Both metrics are based on Elmore's observation that the rise time is proportional to the *radius of gyration* of the area under the impulse response curve (which is essentially the same as the standard deviation of the impulse response). Elmore derived his metric by approximating the *RC* impulse response with a Gaussian distribution, while S2M is derived by approximating

---

[1] The formulation in (14) is not always stable for *RLC* cases. For underdamped *RLC* cases, the impulse response is not a PDF and the square root term in (13) and (14) may become negative.

the step response with a single-pole exponential waveform. Though Elmore's metric may work better for general amplifiers, S2M is more accurate for *RC* circuits. This can be seen by considering a simple lumped *RC* circuit. The response of this simple circuit is a single pole exponential of the form $1 - e^{-(t/RC)}$. Solving this for 10%–90% time yields the same result as obtained using S2M, demonstrating that S2M works better than Elmore's slew metric for *RC* circuits.

The S2M metric is derived by approximating the *RC* step response with a single-pole exponential waveform. This approximation works very well for far-end nodes. However, at near-end nodes, it can cause high errors in slew estimation because the actual response can deviate greatly from a single-pole exponential approximation. Similarly, Elmore's metric also fails at near-end nodes because its fundamental approximation of modeling the impulse response as a Gaussian distribution is highly inaccurate for these nodes. It has been shown that near-end *RC* impulse responses are nonsymmetric [12] and hence cannot be approximated as simple symmetric Gaussian distributions. One approach to extend S2M to near-end nodes is by considering higher order approximations (like AWE). Similarly, Elmore's metric can be extended to near-end nodes by fitting the impulse response to more complex distributions (like Weibull, h-gamma, or lognormal) instead of a Gaussian distribution. Both these approaches have been implemented and are shown to be highly accurate. Their drawback is that we lose the simplicity and efficiency of S2M or Elmore-type metrics and hence these approaches find limited use in physical design optimizations.

To address the above issue, we now describe a metric that is accurate even for near-end nodes while retaining the simplicity of S2M. This new metric is called *scaled S2M*. This metric is developed based on the observed similarities of S2M as a slew metric and scaled Elmore $(= \ln 2 * \mathrm{Elmore})$ as a 50% delay metric. Both these metrics are single-pole approximations of an *RC* response and can be derived by matching the second and first central moments of the *RC* impulse response respectively. However, S2M is much more accurate in slew prediction than scaled Elmore is in delay prediction. This is because S2M uses two circuit moments while scaled Elmore is a simpler single moment-based metric. Another similarity in these metrics is that scaled Elmore uses the mean to approximate 50% delay (median) while S2M uses the standard deviation to approximate 10%–90% slew. These approximations are usually accurate for middle- and far-end nodes but do not hold well for near-end nodes that frequently show long tails due to resistive shielding effects. Step responses with long tails translate to impulse responses with long tails and large skewness (third central moment). Since such impulse responses are highly asymmetric, using the mean and standard deviation to approximate the 50% delay and 10%–90% slew becomes inaccurate. Also, near-end impulse response PDFs are highly skewed in the positive direction causing S2M and scaled Elmore to significantly *overestimate* slew and delay at these nodes.

The authors of [10] observed the trend that scaled Elmore significantly overestimates delay at the near-end, while slightly underestimating delay at the far-end. As a result they proposed the D2M metric by introducing an empirical multiplicative factor $r = -m_1/\sqrt{m_2}$ to the scaled Elmore metric. This factor was found to be much less than one for near-end nodes and slightly greater than one for far-end nodes. Using this factor, the accuracy in delay prediction is vastly improved. S2M shows a similar trend of overestimation at the near-end, although it is highly accurate at far-end nodes. Based on these observations relating scaled Elmore as a delay metric and S2M as a slew metric, we propose that a similar factor be used to improve near-end accuracy. This is the basis of a second new slew metric called scaled S2M.

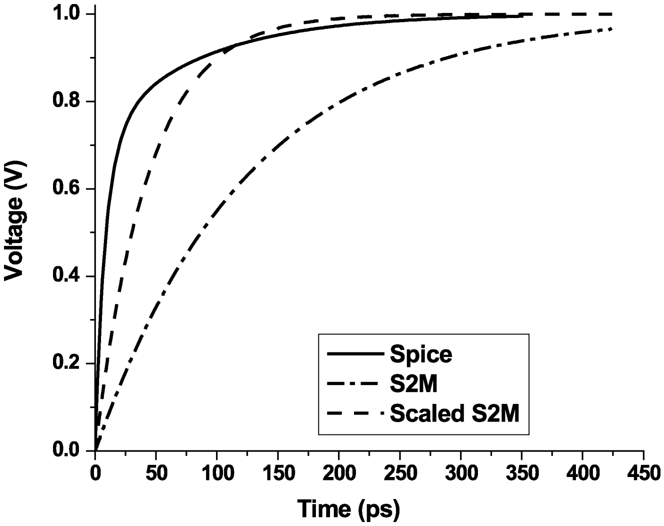

Fig. 3. *RC* circuit response waveform of a difficult near-end node compared to S2M and scaled S2M approximations. Near-end waveforms often show long tails resulting in overestimation of slew by S2M.

Empirically, we have found a good multiplicative factor to be $\sqrt{-m_1/\sqrt{m_2}}$, which is the square root of the factor proposed to improve scaled Elmore in [10]. This is intuitive since S2M is a variance-based metric while scaled Elmore is mean-based. Also, S2M shows better accuracy than scaled Elmore and hence the multiplicative factor for S2M should be less than that for scaled Elmore (i.e., closer to 1). The new scaled S2M metric is given by

$$\text{Scaled S2M} = \frac{\sqrt{-m_1}}{\sqrt[4]{m_2}}(\ln 9)\left(\sqrt{2m_2 - m_1^2}\right). \tag{15}$$

One justification of the multiplicative factor in scaled S2M stems from the observation that near-end impulse responses show long tails. Given an impulse response $h(t)$, ideally, we need to solve the following set of equations for 10% and 90% points.

$$\int_0^{T_{0.1}} h(t)dt = 0.1 \qquad \int_0^{T_{0.9}} h(t)dt = 0.9. \tag{16}$$

The information contained in the probability moments (and hence circuit moments) are

$$\int_0^{\infty} th(t)dt = \hat{m}_1 \qquad \int_0^{\infty} t^2h(t)dt = \hat{m}_2. \tag{17}$$

Note that t does not appear in the integration of (16) while it does in the integration of (17). If we use variance $(\int_0^\infty t^2h(t)dt - (\int_0^\infty th(t)dt)^2)$ to estimate slew, then for an impulse response with a long tail, $th(t)$ and $t^2h(t)$ at high values of t become significant. Variance depends upon the entire distribution and increases with long tails while 10%–90% slew depends only until the point where the area below the curve is 90%. Hence, for slew purposes, the tail of $h(t)$ at very high values of t is not important. Empirically, we found that one way to modify variance and nullify the effect of the tail on variance is by multiplying variance with a function of $((\int_0^\infty th(t)dt)/(\sqrt{\int_0^\infty t^2h(t)dt}))$, which is similar to $m_1/\sqrt{m_2}$. Modifying variance (σ^2) by $m_1/\sqrt{m_2}$ results in a $\sqrt{m_1/\sqrt{m_2}}$ term in standard deviation.

Fig. 3 shows a simulated near-end *RC* response as well as both S2M and scaled S2M approximations. This is a particularly difficult near-end case as seen from the very long tail of the response. It is clear that S2M overestimates slew due to the long tail while scaled S2M shows much better 10%–90% fit for this test case.

Finally, the S2M metric is effectively a scaled form of the standard deviation of the impulse response. The potential relationship between

TABLE I
COMPARISON BETWEEN DIFFERENT SLEW METRICS AT VARIOUS NODES OF A 50 SEGMENT *RC* LINE. SLEW RATES ARE GIVEN IN ps AND ERROR RELATIVE TO SPICE IS GIVEN IN ()

Node	Bakoglu	Elmore	D2M	Weibull	Lognormal	Scaled S2M	S2M	Spice
Near-end	109.8 (-30.4%)	173.2 (9.8%)	77.6 (-50.8%)	132.3 (-16.2%)	143.8 (-8.8%)	160.0 (1.4%)	190.2 (20.5%)	157.8
Node 10	169.1 (-16.1%)	197.1 (-2.2%)	147.3 (-26.9%)	189.4 (-6.0%)	199.0 (-1.3%)	202.0 (0.2%)	216.5 (7.4%)	201.6
Node 20	215.3 (-3.6%)	207.4 (-7.2%)	209.1 (-6.4%)	221.4 (-0.9%)	225.2 (0.8%)	224.6 (0.5%)	227.9 (2.0%)	223.4
Node 30	248.2 (6.9%)	211.2 (-9.0%)	256.5 (10.5%)	238.1 (2.6%)	233.6 (0.6%)	235.8 (1.6%)	232.0 (-0.04%)	232.1
Far-end	274.6 (17.5%)	212.1 (-9.0%)	296.1 (26.6%)	247.4 (5.8%)	235.2 (0.6%)	242.0 (3.5%)	233.0 (-0.4%)	233.8

slew rate and the standard deviation of $h(t)$ has been suggested previously in [2] and [3]. In this work, we provide a theoretical basis for the use of the scaled standard deviation based on the idea that *RC* circuits behave as exponential waveforms and the mapping of this waveform to a CDF. We then develop the scaled S2M metric which is simple yet accurate, even for difficult near-end waveforms. In the following sections, we show results for both S2M and scaled S2M and also test various other slew metrics for the first time; given the current emphasis on 50% delay model accuracy in the literature, we feel that a thorough comparison of slew metrics is needed.

B. Extension to Ramp Inputs

The S2M and scaled S2M metrics can be easily extended to ramp inputs by using the *P*robability distribution function *E*xtension for *R*amp *I*nputs (PERI) approach described in [14]. The PERI technique is based on the fact that when two mutually independent PDFs are convolved, their mean and central moments add. By using this simple observation, the authors of [14] propose the following expression to extend step slew metrics to ramp inputs:

$$\text{Slew(Ramp)} = \sqrt{\text{Slew}^2(\text{step}) + T_R^2}. \tag{18}$$

Here, T_R is the input slew and Slew(step) and Slew(ramp) denote slew for step and ramp excitation respectively.

C. Application to RLC Circuits

S2M uses the probability interpretation of an *RC* response and models the step response as a CDF and impulse response as a PDF. Since any monotonic function that satisfies the requirements in (9) can be modeled as a CDF, all overdamped and critically damped *RLC* responses can be captured by the new metrics.

It is well known that inductance results in faster slews [17]. This is due to the fact that when a positive voltage is applied to an inductor, it takes some time to build up the current. Once the current is established, however, it is then continuously supplied for some duration, resulting in overall faster transition times. This effect is captured by S2M and scaled S2M and can be explained by the second circuit moment m_2. Equation (6) shows that m_2 decreases as inductance grows and thus the variance of the impulse response reduces, resulting in faster slew rates.

To avoid the application of S2M and scaled S2M when it does not hold (i.e., underdamped *RLC* cases), the following criteria from [16] can be used to check whether an *RLC* response is overdamped, critically damped, or underdamped:

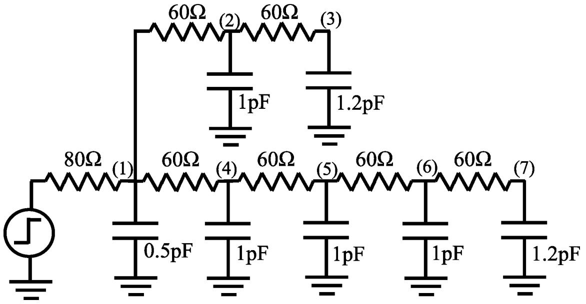

Fig. 4. Simple *RC* tree.

$$\begin{aligned} &4m_2 - 3m_1^2 < 0, && \text{Underdamped} \\ &4m_2 - 3m_1^2 = 0, && \text{Critically damped} \\ &4m_2 - 3m_1^2 > 0, && \text{Overdamped.} \end{aligned} \tag{19}$$

We note that $2m_2 - m_1^2$ is always positive for overdamped and critically damped responses. Indeed, there exist underdamped cases for which S2M and scaled S2M remain stable but this is not globally true and as such these metrics cannot be applied to general underdamped *RLC* systems.

IV. EXPERIMENTAL RESULTS

In this section, we present experimental results for S2M and scaled S2M on a variety of test cases. We compare our results with Elmore's metric $(2 * \text{standard deviation})$, Bakoglu's metric $(\ln 9 * \text{Elmore})$, the Lognormal metric, and also with other delay metrics that can be extended to compute slew. Among major delay metrics, only D2M and Weibull are readily extendable to slew. Though h-gamma can also be extended to compute slews it requires extra look-up tables for 10% and 90% points and the generation of these tables is nontrivial. Hence, we do not compare our results with h-gamma. D2M is altered to model slew rates based on a single-pole approximation as described in [10] while Weibull can be retargeted to 10%–90% delay by solving the Weibull CDF for 10% and 90% points. We draw our preliminary example circuits from prior literature in delay metric analysis for consistency and then consider nets taken from an industrial microprocessor design.

TABLE II
COMPARISON BETWEEN DIFFERENT SLEW METRICS FOR TEST CIRCUIT OF FIG. 4. SLEW RATES ARE GIVEN IN ps AND ERROR RELATIVE TO SPICE IS GIVEN IN ()

Node	Bakoglu	Elmore	D2M	Weibull	Lognormal	Scaled S2M	S2M	Spice
1	1212 (–24%)	1664 (4.2%)	947 (–40.6%)	1426 (–10.5%)	1526 (-4.2%)	1616 (1.3%)	1828 (14.7%)	1594
2	1502 (–12%)	1697 (-0.6%)	1333 (–21.9%)	1663 (–2.6%)	1700 (-0.4%)	1757 (2.9%)	1865 (9.3%)	1707
3	1661 (–3.7%)	1704 (-1.2%)	1559 (–9.6%)	1762 (2.1%)	1751 (1.5%)	1813 (5.1%)	1872 (8.5%)	1725
4	1766 (–10.8%)	1871 (-5.5%)	1628 (–17.8%)	1902 (–3.9%)	1972 (-0.4%)	1973 (–0.3%)	2055 (3.8%)	1980
5	2188 (1.4%)	1957 (-9.3%)	2207 (2.3%)	2164 (0.3%)	2170 (0.5%)	2159 (0%)	2149 (–0.4%)	2158
6	2478 (11.8%)	1985 (-10.4%)	2631 (18.7%)	2288 (3.2%)	2218 (0.1%)	2247 (1.3%)	2180 (–1.6%)	2216
7	2636 (18.6%)	1990 (-10.5%)	2870 (29.1%)	2340 (5.3%)	2227 (0.2%)	2281 (2.6%)	2186 (–1.7%)	2223

A. *RC Line Test Case*

First, we consider an *RC* line with a total line resistance of 150 Ω and a total line capacitance of 1 pF. The driver resistance was chosen to be 50 Ω. The line was modeled as 50 segments. We look at several intermediate nodes along the line. Table I shows the comparison between different slew metrics at various nodes in this 50 segment *RC* line. The table shows that Scaled S2M outperforms all other metrics at near-end nodes while S2M gives the best results at the far-end nodes for this testcase.

B. *RC Tree Test Case*

We consider an *RC* tree taken from [10] and [13] and shown in Fig. 4. Table II shows the comparison between different slew metrics for this test case. S2M results match well with SPICE with very high accuracy at far-end nodes but relatively larger errors at near-end. One interesting comparison is between S2M and Elmore. S2M has a larger constant of proportionality $(\ln 9 = 2.19)$ as compared to Elmore's constant of 2. Hence, the slew numbers predicted by Elmore are always smaller than those predicted by S2M. For far-end nodes, S2M is highly accurate but Elmore underestimates slew by around 10% (which is approximately the percentage difference between 2.19 and 2). This result justifies the claim that Elmore's assumption of a Gaussian distribution is not completely valid for *RC* circuits. Among other metrics, the proposed scaled S2M metric works well for all nodes including very small errors at the near-end. Weibull also matches well with SPICE but underestimates the near-end node slews by over 10%. The Lognormal metric works very well across all nodes; this is somewhat expected in that this metric is significantly more complex than the others and uses different expressions for near, mid, and far-end nodes. Also, the Lognormal metric uses three moments as compared to scaled S2M which is based only on two moments.

C. *RLC Line Test Case*

We consider a 2000-μm distributed *RLC* line taken from [12] and shown in Fig. 5 for this experiment. The line is driven by a step input and the driver resistance is varied to control the damping of the system. The line was modeled by 30 lumped *RLC* segments in SPICE to represent a distributed line. For a particular value of the source resistance R_s, both the *RC* and *RLC* responses are compared with S2M and scaled S2M. It is clear from Table III that *RLC* slews are much smaller than corresponding *RC* slews (by 10%–30% in this case) and that this effect of inductance is accurately modeled by both of the new metrics.

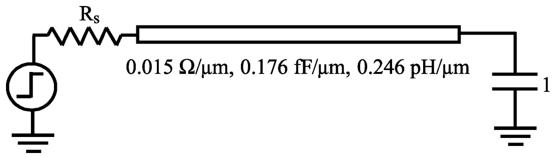

Fig. 5. Uniform distributed *RLC* line.

TABLE III
COMPARISON BETWEEN PROPOSED METRICS AND SPICE FOR TEST CIRCUIT OF FIG. 5. SLEW RATES ARE IN UNITS OF ps AND ERROR RELATIVE TO SPICE IS GIVEN IN ()

	RLC			RC		
	SPICE	S2M	Scaled S2M	SPICE	S2M	Scaled S2M
R_s=65Ω	182	185 (1.6%)	189 (3.8%)	200	200 (0%)	200 (0%)
R_s=55Ω	150	153 (2%)	157 (4.6%)	170	170 (0%)	170 (0%)
R_s=45Ω	117	119 (1.7%)	124 (5.9%)	141	141 (0%)	141 (0%)
R_s=35Ω	82.2	81.7 (–0.6%)	87 (5.8%)	111	111 (0%)	111 (0%)
R_s=25Ω	Underdamped			81	81 (0%)	81 (0%)

D. *Results on Industrial Nets*

We tested the new S2M and scaled S2M metrics on a large number of *RC* interconnect examples from a 0.18-μm high-performance microprocessor design. The total number of nets considered was 6842. These nets were extracted using a commercial extraction tool and represent the most critical and challenging nets for delay calculation. The nodes in each of these nets were classified into near, mid, and far-end nodes. We used the same criteria as in [13] for classifying a node as near, mid, or far-end. Namely, if the 50% delay of a node is less than or equal to 25% of the maximum delay of any node in that net, then the node is classified as a near-end node. If the delay of a node falls between 25% and 75% of the maximum delay, then it is a mid-end node.

TABLE IV
ERROR STATISTICS OF SLEW METRICS ON NEAR, MID AND FAR-END NODES OF 6842 NETS TAKEN FROM A 0.18-μm HIGH-PERFORMANCE INDUSTRIAL MICROPROCESSOR

		Bakoglu	**Elmore**	**D2M**	**Weibull**	**Lognormal**	**Scaled S2M**	**S2M**
4093 near-end nodes	**Mean**	23.7%	32.5%	46.8%	11.7%	7.8%	9.5%	31.3%
	Std Deviation	9.7%	45.6%	6.8%	10.9%	11.6%	10.2%	18.8%
12352 mid-end nodes	**Mean**	10.9%	4.5%	18.7%	3.8%	1.3%	1.4%	6.4%
	Std Deviation	7.5%	4.2%	12.4%	3.4%	1.6%	1.6%	4.5%
65250 far-end nodes	**Mean**	9.5%	8.2%	14.8%	3.5%	0.8%	1.7%	1.7%
	Std Deviation	11.5%	3.4%	18.2%	4.2%	1%	2.1%	3.6%

Similarly, the nodes with delay values greater than 75% of the maximum are labeled far-end nodes. We applied Bakoglu, Elmore, D2M, Weibull, Lognormal, S2M, and scaled S2M to all nodes and computed error relative to SPICE. The near-end nodes are the most difficult for delay and slew metrics while the far-end nodes are relatively easy to model, hence the performance of the metrics for near, mid, and far-end nodes is discussed separately.

1) Near-End Nodes: The total number of near-end nodes tested was 4093. Table IV shows the mean and standard deviation while Table V provides error bins for the different metrics (errors are taken as absolute values when computing the mean and error bins). Scaled S2M was found to be very accurate with an average error of 9.5%. With scaled S2M, 72% of the total nodes showed less than 10% error. Weibull also performed well at these nodes while S2M, Elmore, Bakoglu and D2M were found to be highly inaccurate. Lognormal was found to be highly accurate with an average error of 7.8%. The standard deviation of error is sometimes used to describe the stability of a metric; using this approach the scaled S2M is slightly more stable than Lognormal but with somewhat higher average error.

Fig. 6 shows stacked histograms of the relative error distributions for the seven metrics. Some important conclusions about near-end nodes can be drawn from these error histograms. First, the results show that the simple variance-based S2M metric highly overestimates slew at near-end nodes. This is because of the long tail in the near-end response as discussed in Section III-A and seen in Fig. 3. Scaled S2M reduces this pessimism and provides much better results. Another important observation is that metrics using a single-pole approximation that were originally focused on 50% delay (Bakoglu and D2M) greatly underestimate slew at near-end nodes. This can also be explained by analyzing the near-end waveform from Fig. 3. It is clear from the figure that any single-pole approximation that attempts to fit the 50% delay point accurately will result in significant underestimation of slew. This supports our argument that metrics developed to capture 50% delay are not well suited to be extended for slew. These results also justify the use of accurate closed-form slew metrics (like scaled S2M) in conjunction with an accurate delay metric (like D2M) to capture the key points of a waveform. Finally, the histograms show that Weibull and Lognormal tend to underestimate slew while the proposed scaled S2M metric generally provides conservative results, which is desirable.

2) Mid-End Nodes: The total number of mid-end nodes tested was 12 352. Table IV shows the statistics of the error distribution and Table V shows error bins for different metrics. Mid-end nodes are easier than near-end nodes and all metrics perform better for these cases. Scaled S2M and Lognormal show similar error statistics. Both perform extremely well with an average error of 1.4% and 1.3%, respectively. These metrics also exhibit small standard deviations indicating their stability from net to net. S2M, which was rather inaccurate for near-end nodes, performs much better on these nodes. Table V also shows that scaled S2M predicts the slew rate of 77% of the nodes within 2% of SPICE.

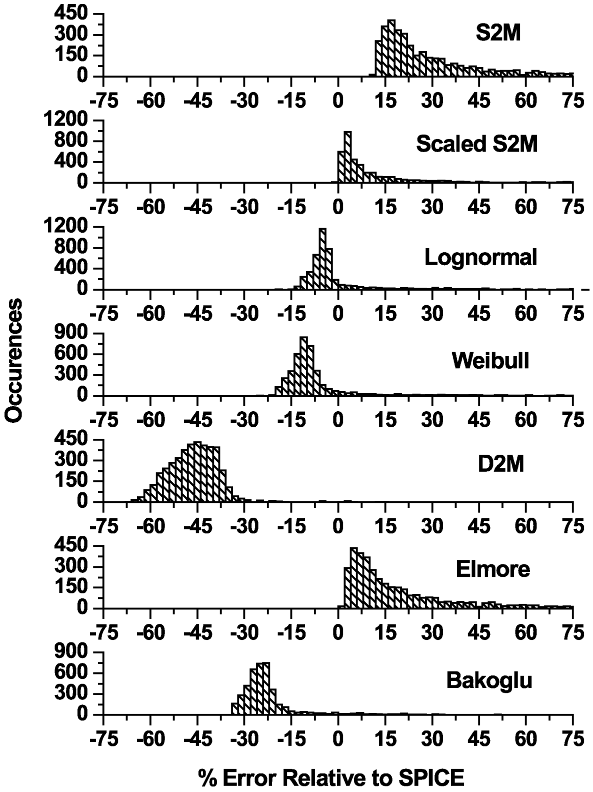

Fig. 6. Error histograms of slew metrics on 4093 near-end nodes taken from nets from an industrial microprocessor design. Histogram bins are set at 5%. Note differing y axis scales.

Fig. 7 shows stacked histograms of relative error distributions for the seven metrics demonstrating that scaled S2M and Lognormal are highly accurate in nearly all cases. S2M and Weibull also perform well while D2M and Bakoglu are inaccurate and unpredictable (indicated by large standard deviations). As was the case for near-end nodes, both S2M and scaled S2M rarely underestimate the actual slew by more than a few percent. While not strict upper bounds as Elmore is for delay prediction, they typically provide conservative results whereas other metrics, including Lognormal and Weibull, can be fairly optimistic. We measured maximum underestimation by different metrics on these 12 352 nodes. The maximum underestimation for S2M and scaled S2M was 0.2% and 2%, respectively, as compared to 55.9% for D2M, 32.7% for Bakoglu, 18.4% for Weibull, 11.9% for Elmore, and 11.8% for Lognormal.

3) Far-End Nodes: The total number of far-end nodes tested was 65 250. Table IV shows the statistics of error distribution and Table V shows error bins for different metrics. The average error of S2M is only

TABLE V

ERROR BINS (SHOWING THE FRACTION OF CASES WITH GIVEN ERRORS) OF SLEW METRICS ON NEAR, MID AND FAR-END NODES OF 6842 NETS TAKEN FROM A 0.18-μm HIGH-PERFORMANCE INDUSTRIAL MICROPROCESSOR

	Error bound	**Bakoglu**	**Elmore**	**D2M**	**Weibull**	**Lognormal**	**Scaled S2M**	**S2M**
4093 near-end nodes	**< 5%**	2.4%	12.6%	0%	8.3%	43.9%	44.8%	0%
	< 10%	5.3%	36.3%	0%	39.4%	82.7%	72%	0%
	< 15%	8.6%	49.9%	0%	80.6%	92.1%	81.4%	10.7%
12352 mid-end nodes	**< 1%**	4.7%	10.9%	2.6%	18.3%	50.1%	50.6%	3.9%
	< 2%	11%	22.8%	5.5%	34.1%	83.8%	76.9%	14.7%
	< 5%	25%	57%	15.2%	67.3%	98.5%	97.5%	45.6%
	<10%	45.7%	98.7%	28.2%	97.5%	99.8%	99.7%	81.2%
65250 far-end nodes	**< 1%**	12.5%	1.1%	10.5%	17.8%	90.5%	32.8%	62.1%
	< 2%	16.7%	2%	14%	32.9%	97.1%	67.2%	74%
	< 5%	31.3%	4.9%	22.4%	70.5%	99.1%	98.9%	93.9%
	<10%	51.3%	96.1%	42.9%	98.8%	99.9%	99.6%	96.6%

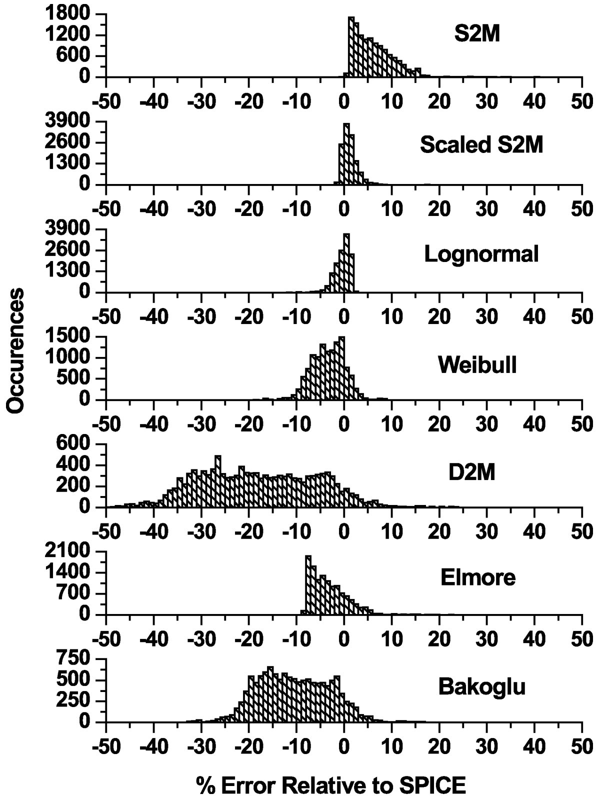

Fig. 7. Error histograms of slew metrics on 12 352 mid-end nodes taken from nets from an industrial microprocessor design. Histogram bins are set at 1%. Note differing y axis scales.

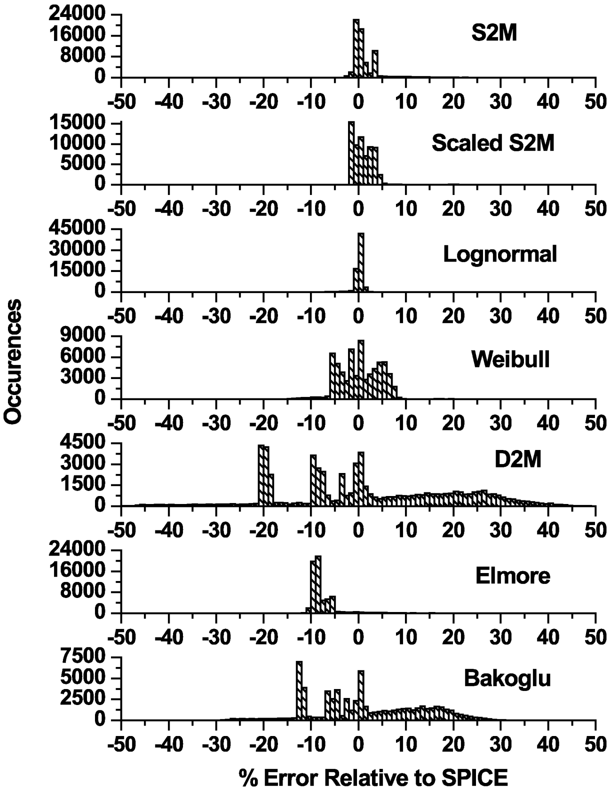

Fig. 8. Error histograms of slew metrics on 65 250 far-end nodes taken from nets from an industrial microprocessor design. Histogram bins are set at 1%. Note differing y-axis scales.

1.7%. Scaled S2M shows the same average error with the smallest standard deviation. Scaled S2M and S2M predictably show comparable results at far-end nodes since the multiplicative factor of scaled S2M is typically very close to one in these cases. Table V shows that scaled S2M predicts the slew rate of 98.9% of the sinks within 5% of SPICE. S2M is also highly accurate with 93.9% of the nets showing less than 5% error.

Fig. 8 shows stacked histograms of relative error distributions for the seven metrics. It is clear that Lognormal, S2M, and scaled S2M are highly accurate at nearly all nodes. Weibull also performs well but its results were found to be as optimistic as 18.5% compared to only 2.1% and 3% worst-case underestimation by scaled S2M and S2M respectively. Elmore's metric shows an average error of around -10%, further demonstrating that for *RC* circuits, the constant of proportionality should be (ln 9) instead of two as proposed by Elmore.

Finally, we examined the 100 far-end nodes with the highest average error among all metrics in an attempt to focus on extremely difficult

TABLE VI
MEAN ERROR OF INDIVIDUAL SLEW METRICS ON THE 100 MOST DIFFICULT FAR-END NODES OUT OF A TOTAL OF 65 250 NODES TAKEN FROM A 0.18-μm HIGH-PERFORMANCE INDUSTRIAL MICROPROCESSOR

Mean Error	**Bakoglu**	**Elmore**	**D2M**	**Weibull**	**Lognormal**	**Scaled S2M**	**S2M**
100 nodes	26.5%	12.3%	46.7%	12%	6.1%	5%	23.4%

cases and ensure that the above results are not skewed by large number of relatively easy nodes. Table VI shows the average error for individual metrics on these 100 nodes. Scaled S2M and Lognormal remain the most accurate metrics when considering the most difficult nodes. S2M (with an average error of only 1.7% while considering all 65 250 far-end nodes) becomes highly inaccurate when only the 100 most difficult nodes are considered. This occurs since the step responses at this subset of nodes deviate significantly from a simple one-pole approximation. At these nodes, the responses show long tails causing large errors in S2M. The newly proposed scaled S2M metric performs extremely well on these difficult testcases with an average error of only 5%, showing better accuracy than the more complex Lognormal distribution.

V. CONCLUSION

This paper describes a new metric to accurately compute the slew rate at any node in an *RC* circuit. The metric scaled S2M is a simple closed-form function of the first two circuit moments that can be computed efficiently using path tracing algorithms. We compare the accuracy of scaled S2M with the Elmore, Bakoglu, and Lognormal slew models and also with extended versions of the D2M and Weibull delay metrics. In general, scaled S2M shows higher accuracy than all other metrics, while being comparable (but slightly less accurate) to the recently proposed Lognormal metric. The advantages of scaled S2M over Lognormal are that it is substantially simpler and tends to give conservative results. On a large set of nets from an industrial microprocessor, scaled S2M predicts the slew rate of 98.9% of the sinks within 5% of SPICE. We further show that metrics relying on a simple constant multiplied by standard deviation, such as S2M and Elmore, do not work well for near-end nodes. The newly proposed scaled S2M metric works well across all nodes with an average error of 9.5% on 4093 traditionally difficult near-end nodes. Furthermore, though this metric is not a general *RLC* slew metric, it can be applied to overdamped and critically damped *RLC* systems while maintaining good accuracy.

We suggest the use of scaled S2M along with the D2M delay metric as both are simple expressions of the same inputs (m_1, m_2). This makes the runtime necessary to compute both slew and 50% delay equal to that of finding 50% delay alone. Also, they act in a complementary manner to provide a high degree of accuracy. The new scaled S2M metric should be useful in a range of physical design areas such as noise avoidance during routing, on-the-fly wire resizing/spacing, and fast checking of slew-rate constraints.

REFERENCES

[1] J. Rubinstein, P. Penfield Jr., and M. A. Horowitz, “Signal delay in *RC* tree networks,” *IEEE Trans. Computer-Aided Design*, vol. CAD-2, pp. 202–211, July 1983.

[2] W. C. Elmore, “The transient response of damped linear networks with particular regard to wideband amplifiers,” *J. Appl. Phys.*, vol. 19, pp. 55–63, 1948.

[3] R. Gupta, B. Tutuianau, and L. T. Pileggi, “The Elmore delay as a bound for *RC* trees with generalized input signals,” *IEEE Trans. Computer-Aided Design*, vol. 16, pp. 95–104, Jan. 1997.

[4] L. T. Pillage and R. Rohrer, “Asymptotic waveform evaluation for timing analysis,” *IEEE Trans. Computer-Aided Design*, vol. 9, pp. 352–366, Apr. 1990.

[5] P. Feldman and R. W. Freud, “Efficient linear circuit analysis by Pade approximation via the Lanczos process,” *IEEE Trans. Computer-Aided Design*, vol. 14, pp. 639–649, May 1995.

[6] A. Odabasioglu, M. Celik, and L. Pileggi, “PRIMA: Passive reduced-order interconnect macromodeling algorithm,” in *Proc. Int. Conf. Computer-Aided Design*, 1997, pp. 58–65.

[7] C. L. Ratzlaff, N. Gopal, and L. T. Pillage, “RICE: Rapid interconnect circuit evaluator,” in *Proc. Design Automation Conf.*, 1991, pp. 555–560.

[8] B. Tutuianu, F. Dartu, and L. Pileggi, “An explicit *RC*-circuit delay approximation based on the first three moments of the impulse response,” in *Proc. Design Automation Conf.*, 1996, pp. 611–616.

[9] A. B. Kahng, K. Masuko, and S. Muddu, “Analytical delay models for VLSI Interconnects under ramp input,” in *Proc. Int. Conf. Computer-Aided Design*, 1996, pp. 30–36.

[10] C. J. Alpert, A. Devgan, and C. Kashyap, “A two moment *RC* delay metric for performance optimization,” in *Proc. Int. Symp. Physical Design*, 2000, pp. 69–74.

[11] R. Kay and L. Pileggi, “PRIMO: Probability interpretation of moments for delay calculation,” in *Proc. Design Automation Conf.*, 1998, pp. 463–468.

[12] T. Lin, E. Acar, and L. Pileggi, “h-gamma: An *RC* delay metric based on a gamma distribution approximation to the homogenous response,” in *Proc. Int. Conf. Computer-Aided Design*, 1998, pp. 19–25.

[13] F. Liu, C. Kashyap, and C. J. Alpert, “A delay metric for *RC* circuits based on the Weibull distribution,” in *Proc. Int. Conf. Computer-Aided Design*, 2002, pp. 620–624.

[14] C. Kashyap, C. J. Alpert, A. Devgan, and F. Liu, “PERI: A technique for extending delay and slew metrics for ramp inputs,” in *Proc. Workshop Timing Issues Dig. Syst.*, 2002, pp. 57–62.

[15] H. B. Bakoglu, *Circuits, Interconnections, and Packaging for VLSI*. Reading, MA: Addison-Wesley, 1990.

[16] Y. I. Ismail, E. G. Friedman, and J. L. Neves, “Equivalent Elmore delay for *RLC* trees,” *IEEE Trans. Computer-Aided Design*, vol. 19, pp. 83–97, Jan. 2000.

[17] ——, “Exploiting the on-chip inductance in high-speed clock distribution networks,” *IEEE Trans. VLSI Syst.*, vol. 9, pp. 963–973, Dec. 2001.

[18] L. T. Pileggi, “Timing metrics for physical design of deep-submicron technologies,” in *Proc. Int. Symp. Physical Design*, 1998, pp. 28–33.

[19] Q. Yu and E. S. Kuh, “Exact moment matching model of transmission lines and application to interconnect delay estimation,” *IEEE Trans. VLSI Syst.*, vol. 3, pp. 311–322, June 1995.

[20] C. Alpert, F. Liu, C. Kashyap, and A. Devgan, “Delay and slew metrics using the lognormal distribution,” in *Proc. Design Automation Conf.*, 2003, pp. 382–385.